

## CHARGE TRANSFER IN THE COLLISION SYSTEM $\text{He}^{2+} + \text{C}_{60}^+$ : THEORY AND EXPERIMENT

H. Bräuning,<sup>1</sup> L. P. Presnyakov,<sup>2</sup> A. A. Narits,<sup>2</sup> A. Diehl,<sup>1</sup> R. Trassl,<sup>1</sup>  
A. Theiß,<sup>1</sup> and E. Salzborn<sup>1</sup>

<sup>1</sup>*Institut für Atom- und Molekülphysik, Justus-Liebig Universität, Leihgesterner Weg 217  
D-35392 Giessen, Germany*

<sup>2</sup>*P. N. Lebedev Physical Institute, Russian Academy of Sciences  
Leninskii Pr. 53, Moscow 119991, Russia*

e-mail: Erhard.Salzborn@strz.uni-giessen.de presn@sci.lebedev.ru

### Abstract

Fullerenes are a direct link between atoms with discrete electronic energy levels and solids with a band structure and a well-defined surface. In this paper, we report on a quantum mechanical treatment of charge transfer and ionization in the ion-ion collision system  ${}^3\text{He}^{2+} + \text{C}_{60}^+$ . This approach considers under- and over-barrier transitions through the one-dimensional barrier between the collision partners. The calculated cross sections for charge transfer compare favorably with experimental data measured in the center-of-mass energy range from 27 to 196 keV employing the crossed beams technique.

**Keywords:** fullerenes, ion-ion collisions, charge transfer, ionization.

Fullerenes have been the subject of intense research within the last 15 years as they offer new opportunities to study the interaction of extended structures. The fundamental processes of electron transfer and ionization have been studied extensively in collision experiments. In addition to the traditional experiments with energetic ions and neutral  $\text{C}_{60}$  molecules [1] as well as with charged fullerene projectiles and neutral targets [2–4] the electron transfer in collisions between two fullerene ions [5] and in collisions between a fullerene ion and a helium ion [6] has been studied recently. In the case of electron transfer, fullerenes are often considered as a conducting sphere with the valence electrons populating very delocalized orbitals. The electrons can therefore move freely on the sphere in a manner that is similar to the free electron movement in the conduction band of a solid. This is reflected in the large dipole polarizability [7] of  $540a_0^3$  ( $a_0$  is the Bohr radius). The importance of polarization in a fullerene target has already been shown using electron-impact ionization of negatively charged fullerene ions [8] and in an earlier work by Shen et al. [4] who proposed a model based on sequential single-electron transfer to explain their measured cross section for double electron capture by  $\text{C}_{70}^{3+}$  from neutral  $\text{C}_{60}$ . Within this model the cross section is determined by the single-electron transfer cross section from the intermediate  $\text{C}_{60}^+$  ion to the intermediate  $\text{C}_{70}^{2+}$  ion and thus by the collision dynamics between two fullerene ions. Expanding on this model, a quantum treatment has been developed [5] which is in very good agreement with experimental cross sections for the resonant reactions  $\text{C}_{60}^{2+} + \text{C}_{60}^+ \rightarrow \text{C}_{60}^+ + \text{C}_{60}^{2+}$  at center-of-mass energies ranging from 27 to 69 keV and, at much lower collision energies,  $\text{C}_{60}^+ + \text{C}_{60} \rightarrow \text{C}_{60} + \text{C}_{60}^+$  [9].

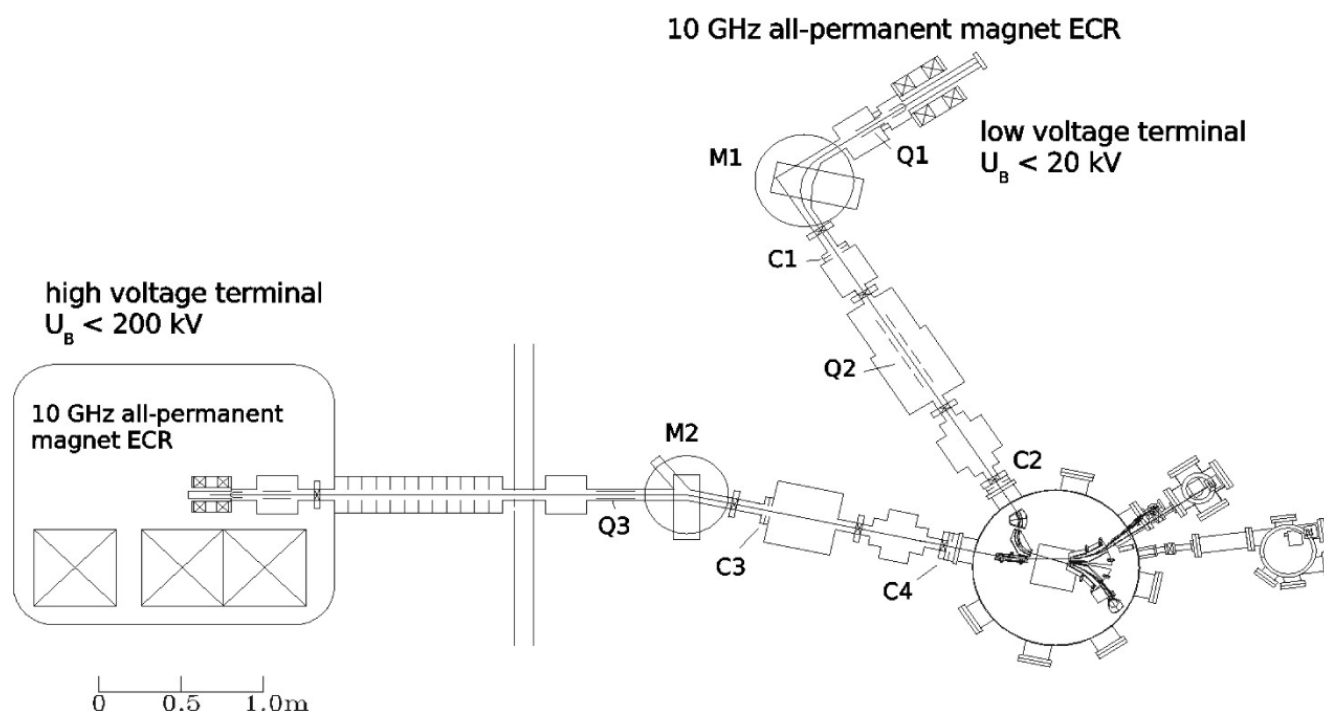


**Fig. 1.** Schematic overview of the Giessen ion-ion experiment [10, 11]: M1 and M2 are analyzing magnets, Q1–Q3 are quadrupole lenses, and C1–C4 are collimators.

In this letter we present the further development of the quantum treatment to the non-resonant collision system  ${}^3\text{He}^{2+} + \text{C}_{60}^+ \rightarrow {}^3\text{He}^+ + \text{C}_{60}^{2+}$ . The theoretical cross sections for charge transfer are compared to recent experimental data [6].

The experimental cross sections have been obtained with the Giessen ion-ion crossed-beams set-up (see Fig. 1). Here, a beam of  $\text{C}_{60}^+$  ions with 3 keV energy is crossed with a beam of  ${}^3\text{He}^{2+}$  ions with energies in the range 40–200 keV under an angle of  $17.5^\circ$ . After charge transfer both collision partners have changed their charge and are separated from the parent beams by electrostatic analyzers. The  $\text{C}_{60}^{2+}$  product ions are detected with a Channeltron detector, whereas the  ${}^3\text{He}^+$  ions are detected with a Micro Channel Plates detector. Beam currents of typically 1–2 nA for the fullerene ions and 50–100 nA for the helium ions resulted in reaction rates on the order of 0.5 per second. The background contribution from the interaction with the residual gas, which even at pressures below  $10^{-10}$  mbar is several orders of magnitude larger, could be strongly suppressed using the time coincidence technique, which provides a powerful tool for signal recovery and gives a clear signal of the electron transfer reaction. Further experimental details are discussed in depth in [6].

Apart from the statistical error of each measurement, the absolute cross section has a systematic error, which is mostly due to the uncertainty in the detector efficiencies. For the data presented in [6] the detector efficiencies have been obtained by measuring cross sections for the reaction  $\text{He}^+ + \text{He}^{2+} \rightarrow \text{He}^{2+} + \text{He}^+$  under the same conditions as for the reaction with the fullerene ions and comparing with previous data by Melchert et al. [12]. This gave a systematic error of 25%. In order to extend the experimental data to lower collision velocities, we have re-measured some of the older data points and directly measured the detector efficiencies by comparing the number of detected ions with the true

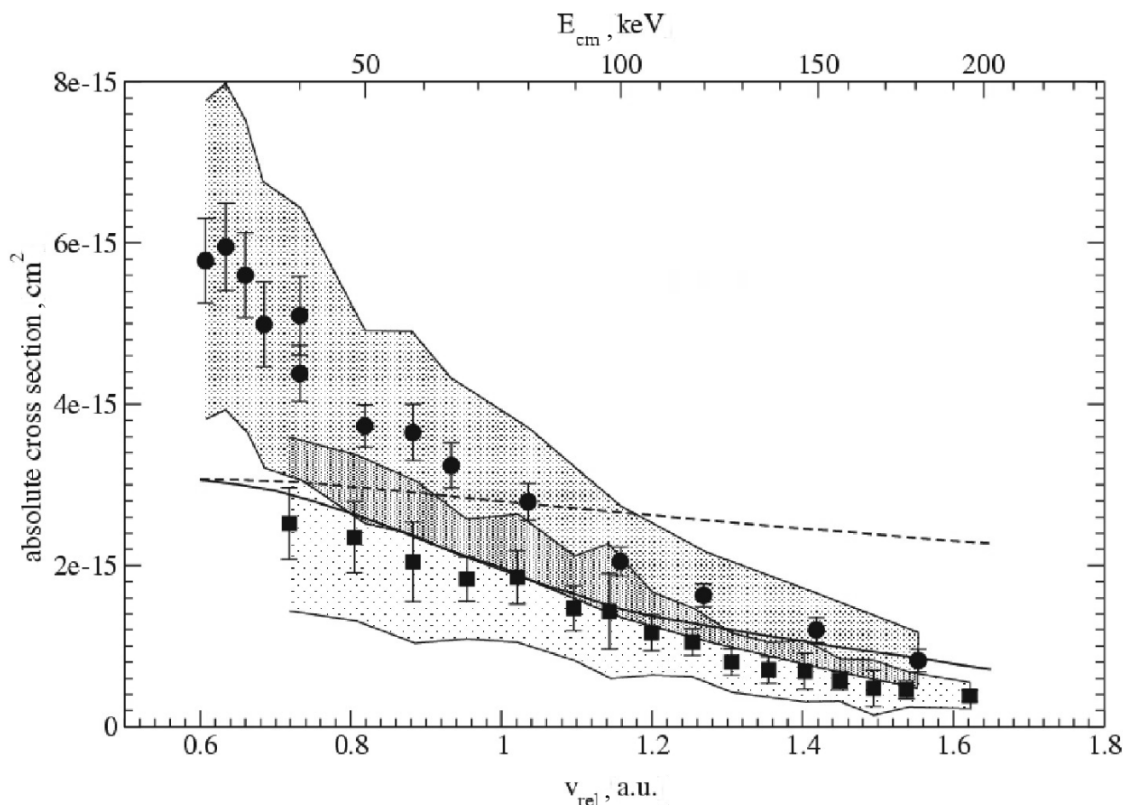


**Fig. 2.** Comparison of the experimental data (squares [6] and circles) for the charge transfer process  ${}^3\text{He}^{2+} + \text{C}_{60}^{+3} \rightarrow \text{He}^+ + \text{C}_{60}^{2+}$  with the theoretical calculations: the dashed curve shows the total electron loss (charge transfer + ionization) and the solid curve, the charge transfer. The error bars represent the statistical error with 90% confidence interval. The shaded areas indicate the total error, including the systematic error of 25% for both measurements.

number of ions in the beam, which is determined by measuring the beam current in a Faraday cup. Due to rate limits on the detectors, this requires the measurement of very low electrical currents on the order of 100 fA and below. This measurement also yields a systematic error of 25% for the absolute cross sections. Figure 2 shows both measurements together with the systematic error as indicated by the shaded areas. Given the significant overlap between the total errors (dark shaded area in Fig. 2), both data sets are found to be in agreement. Our new data have been extended to the lower limit of the collision velocity obtainable by the present set-up. It indicates a strong increase in the cross section with decreasing collision velocity.

Besides the experimental data, Fig. 2 shows the calculated cross sections. As in our previous paper [5], we consider the electron transition as the under- and over-barrier passing of the active electron along the axis between the centers of the projectile and target. For this purpose we evaluate the one-dimensional Schrödinger equation

$$\left\{ \frac{d^2}{dz^2} + \frac{2m_e}{\hbar^2} (E(R) - U(R|z)) \right\} \psi(R|z) = 0. \quad (1)$$

Here,  $\hbar$  is the Planck constant,  $m_e$  is the electron mass, and  $E(R)$  is its binding energy including the

static Stark shift. The distance  $R = R(v_{\text{rel}}, b, t)$  between the center of the fullerene ion and the helium ion is considered as a given function of time  $t$ , impact parameter  $b$ , and relative velocity  $v_{\text{rel}}$  of the colliding particles. In collisions of non-identical particles the potential barrier

$$U(R|z) = e^2 \left[ -\frac{q_1}{R-z} - \frac{q_2}{z} + \frac{q_1 a}{Rz-a^2} - \frac{q_2 a}{Rz} + \frac{1}{2} \left( \frac{a}{z^2} - \frac{a}{z^2-a^2} \right) \right] \quad (2)$$

is not symmetric, having a simpler form than the one between two fullerene ions [13]. Here  $e$  is the electron charge,  $q_1$  and  $q_2$  are the charge states of the helium and fullerene ion cores respectively,  $z$  is the position of the active electron with respect to the center of the fullerene ( $a < z < R$ ), and  $a$  is the radius of the fullerene. With the collision system discussed here, we have  $q_1 = 2$  and  $q_2 = 2$ . For this asymmetric barrier, we have to solve two independent sets of phase and amplitude equations of the form [14, 15]

$$\frac{d\delta}{dx} = -\frac{2V}{k} \sin^2(kx + \delta), \quad \delta(0) = 0, \quad (3)$$

$$\frac{dm}{dx} = m \frac{V}{k} \sin(2kx + 2\delta), \quad m(0) = 1, \quad (4)$$

$$\frac{d\gamma}{dx} = -\frac{2V}{k} \cos^2(kx + \gamma), \quad \gamma(0) = 0, \quad (5)$$

$$\frac{dn}{dx} = -n \frac{V}{k} \sin(2kx + 2\delta), \quad n(0) = 1 \quad (6)$$

in a symmetric interval  $-x_0 \leq x \leq x_0$  with  $x_0 = \frac{R-a}{2}$  and  $x = z - \frac{R+a}{2}$ . As in [5] the energy values in Eq. (1) were taken relative to the bottom of the potential well using  $k^2 = k^2(R) = \frac{2m_e}{\hbar^2} (E(R) + U_0)$  and  $2V(R|x) = \frac{2m_e}{\hbar^2} (U(R|x) + E_0)$ . The choice of the value  $U_0 = 8.44$  Ry results from the numerical evaluation of phase equations (3) and (5) and has been explained in detail in [5]. Equations (4) and (6) for the amplitudes can be integrated if phase equations (3) and (5) are solved. The expressions for the transition coefficient  $T(x_0)$  and the reflection coefficient  $Q(x_0)$  in terms of the phase and amplitude functions are given by

$$T(x_0) = e^{-i[(x_0)+\gamma(x_0)]} \frac{2 \cos[\delta(x_0) - \gamma(x_0)]}{\frac{m(-x_0)}{m(x_0)} e^{i[\delta(-x_0)+\delta(x_0)]} + \frac{n(-x_0)}{n(x_0)} e^{i[\gamma(-x_0)+\gamma(x_0)]}}, \quad (7)$$

$$Q(x_0) = \frac{e^{i[\delta(-x_0)-\delta(x_0)]} - \frac{m(x_0)}{m(-x_0)} \frac{n(-x_0)}{n(x_0)} e^{i[\gamma(-x_0)-\gamma(x_0)]}}{e^{i[\delta(-x_0)+\delta(x_0)]} + \frac{m(x_0)}{m(-x_0)} \frac{n(-x_0)}{n(x_0)} e^{i[\gamma(-x_0)+\gamma(x_0)]}}. \quad (8)$$

By integrating the transmission coefficient  $T(x_0)$  over all values of  $t$  with the help of the so-called decay model [16], the electron loss probability is obtained:

$$P(v_{\text{rel}}, b) = 1 - \exp \left\{ - \int_{-\infty}^{\infty} \omega \left| T \left( \frac{R(v_{\text{rel}}, b, t) - a}{2} \right) \right|^2 dt \right\}. \quad (9)$$

Here,  $\omega$  is the number of the active electron hits against the barrier per unit time. Our estimates show that  $0.95 \leq \omega \leq 1.05$ . The integral should be evaluated over the hyperbolic Coulomb trajectory. In order to use the general quantum mechanical analysis, we employ the correspondence principle that connects the impact parameter  $b$  with the orbital quantum number  $l$  of the relative motion for large  $l$ :  $Mv_{\text{rel}}b = \hbar l$ . Here,  $M$  is the reduced mass of the collision system. The barrier transition probability (9) then corresponds to the scattering matrix element for the electron loss process at the given orbital momentum  $l$ :

$$P(v_{\text{rel}}, b) = |S_{if}(l)|^2. \quad (10)$$

It is worth noting that the characteristic values of the orbital momentum are rather large with  $l \approx 10^4$ . The total cross section for electron loss is equal to

$$\sigma = \pi a_0^2 \left( \frac{m_e v_0}{M v_{\text{rel}}} \right)^2 \sum_l (2l + 1) |S_{if}(l)|^2, \quad (11)$$

where  $a_0 = 0.529 \cdot 10^{-8}$  cm is the Bohr radius and  $v_0 = 2.19 \cdot 10^8$  cm/s is the atomic unit of velocity. The quantal form (11) may be more suitable in some respects than the semiclassical one, especially for the analysis of the angular-differential cross sections.

The barrier model describes the total probability and the cross sections for both processes, charge transfer and ionization. At low relative velocities  $v_{\text{rel}}$ , charge transfer dominates. For medium velocities the contributions from ionization become comparable, and in the limit of large velocities the electron loss is mostly due to ionization. The distribution of the cross sections among the competing channels was discussed by Presnyakov and Uskov [17, 18] for barrier transitions with the help of the Keldysh model [19]. Detailed calculations by Uskov et al. [20] show that the contributions from charge transfer  $\sigma_c$  can be approximated by the expression

$$\frac{\sigma_c}{\sigma_{\text{total}}} = \frac{(2E_i)^{3.26}}{\left(2E_i + \frac{v_{\text{rel}}^2}{4}\right)^{3.26}},$$

where the ionization potential of the fullerene ion  $E_i$  and the relative velocity  $v_{\text{rel}}$  are taken in atomic units. In our calculations we used the following parameters: the radius of  $\text{C}_{60}^+$  and  $\text{C}_{60}^{2+}$  is the same and identical to 8.2 a.u. [21] and the ionization potential of  $\text{C}_{60}^+$  is equal to 12.25 eV [22].

The calculated cross sections for charge transfer are shown in Fig. 2 in comparison with the experimental data. As can be expected for charge transfer in non-resonant collision systems, the experimental cross sections show a significant dependence on the collision velocity. This dependence is fairly well reproduced by the respective calculated cross sections. The theoretical values are in fair agreement with the experimental data at collision velocities above approximately 1 a.u. At lower velocities, the measured cross sections show a strong increase with decreasing velocity. While this is also indicated by theory, the theoretical values show a much more shallow increase. Below a collision velocity of about 0.7 a.u. the experimental data indicate a very sharp increase of the cross section, whereas the theoretical values seem to indicate a flat dependence. However, at these low collision velocities, the cross section for charge transfer may be influenced by electronic excitation or plasmon excitation of the fullerene ion, as it is produced in the hot plasma of the ECR ion source.

Also shown in Fig. 2 is the calculated cross section for the total loss of one electron by the fullerene ion. The difference between the cross sections for total loss and charge transfer directly gives the ionization

cross section. At low collision velocities the ionization cross section is negligible and electron loss is mostly due to charge transfer. However, while the charge transfer cross section decreases strongly with increasing collision velocity, the ionization cross section increases. This results in a relatively weak dependence of the total electron loss cross section on the collision velocity in the considered velocity range. So far, there is no experimental data for the total electron loss. Such experiments are difficult, because the coincidence technique for signal recovery is not applicable. Employing the pulsed-beams technique for signal recovery, the high background in combination with the low signal rate results in large statistical errors or unreasonable long measurement times. Given the predicted large cross section, however, such experiments might become feasible in the near future.

## Acknowledgments

This work was supported by BMBF/GSI and DFG. L.P.P. and A.A.N. gratefully acknowledge support from the Russian Foundation for Basic Research (Grant No. 02-02-16274) and the Russian Federal Program “Intergracia.”

## References

1. B. Walch, C. L. Cocke, R. Voelpel, and E. Salzborn, *Phys. Rev. Lett.*, **72**, 1439 (1994).
2. P. Hvelplund, L. H. Andersen, H. K. Haugen, et al., *Phys. Rev. Lett.*, **69**, 1915 (1992).
3. P. Hvelplund, L. H. Andersen, C. Brink, et al., *Z. Phys. D*, **30**, 323 (1994).
4. H. Shen, P. Hvelplund, D. Amthur, et al., *Phys. Rev. A*, **52**, 3847 (1995).
5. H. Bräuning, R. Trassl, A. Diehl, et al., *Phys. Rev. Lett.*, **91**, 168 (2003).
6. H. Bräuning, R. Trassl, A. Diehl, et al., *Physica Scripta*, **T110**, 355 (2004).
7. A. Scheidemann, V. Kresin, and W. Knight, *Phys. Rev. A*, **49**, R4293 (1994).
8. P. Scheier, D. Hathiramani, W. Arnold, et al., *Phys. Rev. Lett.*, **84**, 55 (2000).
9. F. Rohmund and E. E. B. Campbell, *J. Phys. B: At. Mol. Opt. Phys.*, **30**, 5293 (1997).
10. F. Melchert and E. Salzborn, “Charge changing processes in ion–ion collisions,” in: Y. Itikawa (ed.), *The Physics of Electronic and Atomic Collisions (Sendai, 1999)*, AIP Conference Proceedings, Woodbury, New York (2000), Vol. 500, p. 478.
11. S. Meuser, F. Melchert, S. Krüdener, et al., *Rev. Sci. Instr.*, **67**, 2752 (1996).
12. F. Melchert, S. Krüdener, R. Schulze, et al., *J. Phys. B: At. Mol. Opt. Phys.*, **28**, L355 (1995).
13. H. Zettergren, H. T. Schmidt, H. Cederquist, et al., *Phys. Rev. A*, **66**, 032710 (2002).
14. L. P. Presnyakov, *Phys. Rev. A*, **44**, 5636 (1991).
15. L.P. Presnyakov, “Wave propagation in homogeneous media,” in: E. Wolf (ed.), *Progress in Optics*, Elsevier, Amsterdam (1995), Vol. 34, p. 159.
16. R. Janev, L. P. Presnyakov, and V. Shevelko, *Physics of Highly Charged Ions*, Springer Verlag, Berlin (1986).
17. L. P. Presnyakov and D. B. Uskov, *Sov. Phys. – JETP*, **59**, 515 (1984).
18. L. P. Presnyakov and D. B. Uskov, “Charge transfer and ionization at atomic collisions,” in: I. I. Sobelman (ed.), *Proceedings of the P. N. Lebedev Physical Institute*, Nova Science Publishers, New York (1987), Vol. 179, p. 137.
19. L. V. Keldysh, *Sov. Phys. – JETP*, **20**, 1307 (1965).

20. D. B. Uskov, J. Botero, R. K. Janev, and L. P. Presnyakov, "Cross Sections of Electron Capture and Ionization in Collisions of Fusion Plasma Impurity Ions with Atomic Hydrogen," *Report INDC(NDS)-291*, IAEA, Vienna (1993), Vol. 291.
21. H. Cederquist, A. Fardi, K. Haghighat, et al., *Phys. Rev. A*, **61**, 022712 (2000).
22. C. Lifshitz, M. Iraqi, T. Peres, and J. E. Fischer, *Rapid Commun. Mass Spectrom.*, **5**, 238 (1991).